RSC Advances

PAPER

View Article Online
View Journal | View Issue

Cite this: *RSC Adv.*, 2024, **14**, 24671

Coumarin–amino acid hybrids as promising anticancer agents: design, synthesis, docking studies and CK2 inhibition†

Abd-Allah S. El-Etrawy,[ab] Ahmad Ramadan,[c] Farag F. Sherbiny, *[d] I. F. Zeid,[c] A. A.-H. Abdel-Rahman[c] and Mohamed A. Hawata[c]

A series of mono-peptide, di-peptide and tri-peptide derivatives linked to a coumarin scaffold (**5a–c**, **7a–c**, and **9a–c**) were synthesized *via* the azide-coupling method from corresponding hydrazides **4**, **6**, and **8**. These compounds were tested for anticancer activity against HepG-2, PC-3, and Hct-116 cell lines. Compounds, **7c**, and **5b** showed significant cytotoxicity, outperforming doxorubicin, with IC_{50} values of 34.07, 16.06, and 16.02 μM for **7c** and 42.16, 59.74, and 35.05 μM for **5b**. Compound **7b** also displayed promising results with IC_{50} values of 72.13, 70.82, and 61.01 μM. Moreover, the key structural features of amino acids indicated that mono-peptide and di-peptide derivatives play a key role in increasing their anticancer activities compared with tri-peptides. In addition, the most potent compound **5b** also exhibited strong CK2 kinase inhibition with an IC_{50} value of 0.117 ± 0.005 μM compared with roscovetine as a control drug with an IC_{50} value of 0.251 ± 0.011 μM. Finally, the binding mode of the chemical inhibitors at the active site of CK2 receptor was also investigated using a docking study which confirmed that the presence of the amino acid functionality is an important feature for anticancer activity and the synthesized compounds showed favorable ADME properties. Besides that, SAR analysis was implemented for the target compounds.

Received 9th June 2024
Accepted 12th July 2024

DOI: 10.1039/d4ra04226c

rsc.li/rsc-advances

1 Introduction

For the time being, cancer is considered one of the leading causes of mortality worldwide and therefore, the evolution of potent and robustly effective anticancer agents is one of the most important challenges in advanced therapeutics due to the unique pathophysiology of tumors, systemic toxicity, and the prospective emergence of resistance to chemical therapy.[1] Traditional methods for cancer medication encompass radiotherapy, immunotherapy, chemotherapy, and cancer starvation therapy each with their own limitations.[2]

Heterocyclic compounds are known as interesting scaffolds to incorporate bioactive small molecules, due to their crucial roles in many physiological processes.[3] In this context, coumarins have several attractive chemical features, such as low molecular weight, high solubility, high bioavailability, and low toxicity. Therefore, prosperous coumarin structures have been widely used as an effective template for drug discovery due also to their abilities to interact with many diverse enzymes and receptors and their anticancer properties on diverse cancerous cells.[4] In addition, the versatility of coumarin scaffold has been of great interest because of their potential roles in preventing and treating various diseases.[5] Many products contain coumarin derivatives exhibit a plethora of pharmacological effects including antioxidant,[6,7] carbonic anhydrase inhibitor,[8,9] antibacterial activity,[10] antifungal activity,[11,12] antiviral activity,[13,14] anti-inflammatory activity,[15,16] neuro-protection,[17] anti-convulsant activity,[18,19] anti-coagulant activity,[20,21] as well as anti-diabetic activity,[22,23] and anti-cancer activity.[24,25]

On the other hand, amino acid conjugations are pharmacological agents strategically used to improve water solubility and enhance the anti-cancer activity.[26] Thus, coumarin derivatives containing amino acid are worthy target as the coumarin moiety allows them to be used as fluorescent probes.[27,28] In addition, several amino acids bearing heterocyclic moieties are reported as highly potential antitumor agents.[29–31]

Molecular hybridization of two or more bioactive pharmacophores is a tremendous strategy for drug discovery to give new chemical entities with various and new biological activities.[32,33] In the present study, we assumed that the merging of coumarin

[a]*Department of Chemistry, Basic Science Center, Misr University for Science and Technology (MUST), Al-Motamayez District, 6th of the October City 77, Egypt*
[b]*Department of Pharmaceutical Organic Chemistry College of Pharmaceutical Science & Drug Manufacturing, Misr University for Science and Technology (MUST), Al-Motamayez District, 6th of the October City 77, Egypt*
[c]*Department of Chemistry, Faculty of Science, Menoufia University, Shebin El-Koam, Egypt*
[d]*Pharmaceutical Organic Chemistry Department, Faculty of Pharmacy (Boys), Al-Azhar University, Cairo 11884, Egypt. E-mail: dr-farag-sherbiny@azhar.edu.eg*

† Electronic supplementary information (ESI) available. See DOI: https://doi.org/10.1039/d4ra04226c

nucleus and amino acid moieties in a single chemical structure was able to drive new potential anticancer drug candidate.

Therefore, this study has been focused on the development of coumarin derivatives with particular amino acid residues which may led to novel hybrid compounds with potential anticancer agents. Thence, the synthesized compounds have been examined for their cytotoxic effects against a panel of human cancer cell lines using MTT assay technique and the most potent compounds were further selected and evaluated for their activities against CK2 kinase inhibitors. In addition, the molecular docking was applied to evaluate the binding modes of examined synthesized compounds.

1.1. Rational drug design

Coumarin is an aromatic compound that has a bicyclic chemical structure with lactone moiety. The presence of an electronegative atom is substantially effective for hydrogen bonding interactions and enhancing solubility. Besides, aromatic ring is responsible for having hydrophobic and aromatic stacking interactions as well as the lactone form is responsible for its anticancer activity.[34] The substitution of coumarin nucleus makes its more significant and effective for bioactivity. Abundant types of coumarins have been synthesized and also are present in nature. Different chemical structures of coumarins have been produced due to the various types of substitution patterns or pharmacophoric features in their basic bicyclic structures which are significant in showing effective and diverse classes of biological activities (Fig. 1). The anticancer properties of coumarin derivatives have also been extensively investigated in several studies which are closely related to its anticancer activity.[35–40]

Many SAR studies proposed that the substitution at the 7-position of coumarin moiety are likely promising structural features to obtain excellent antitumor activities[38–42] including many clinical trials or drugs have already been used in the treatment of various cancers.[43,44] In addition, it was found that the cytotoxic properties of substituted coumarins depend on the length of the chain, which increases the lipophilicty and thus facilitating their penetrations into the cells. SAR studies also demonstrated that the linker between coumarin nucleus and the substituent at the 7-position influences the anticancer activity.[44] Moreover, the presence of hydrogen bonding acceptors and donors are essential for their anticancer activities.[45]

On the other hand, the incorporation of coumarin moiety into the side chain of amino acid is expected to improve the achievement of anticancer activity and reduce their adverse side effects. Furthermore, amino acid ester pro-drugs significantly improve the cellular uptake of the parent drugs *via* peptide transport mechanism and some epithelial cancer cells are wealthy in these transporters permits their use for the delivery of peptidomimetic anticancer agents.[46,47] Also, amino acid ester decreases extensive degradation of anti-proliferative chemical drugs which increase their affinity to oligopeptide transports that are overexpressed in the tumor cells.[48] Therefore, L-amino acids are used to design the amino acid pro-drugs therapy.

On the other hand, modern researches have been demonstrated that 7-hydroxycoumarin derivatives inhibit the secretion of cyclin D1, which is overexpressed in abundant types of cancer cells[49–51] and thus could be successfully utilized in cancer therapy. Therefore, the essential core of rational design was prepared by chemical pharmacophoric modifications including the substitution at the 7-position of coumarin moiety with amino acid residues namely, glycine, phenyl glycine and leucine having hydrophobic side chains. Furthermore, the derivatization procedure including formation of mono-peptide, di-peptide and tri-peptide derivatives as chemical

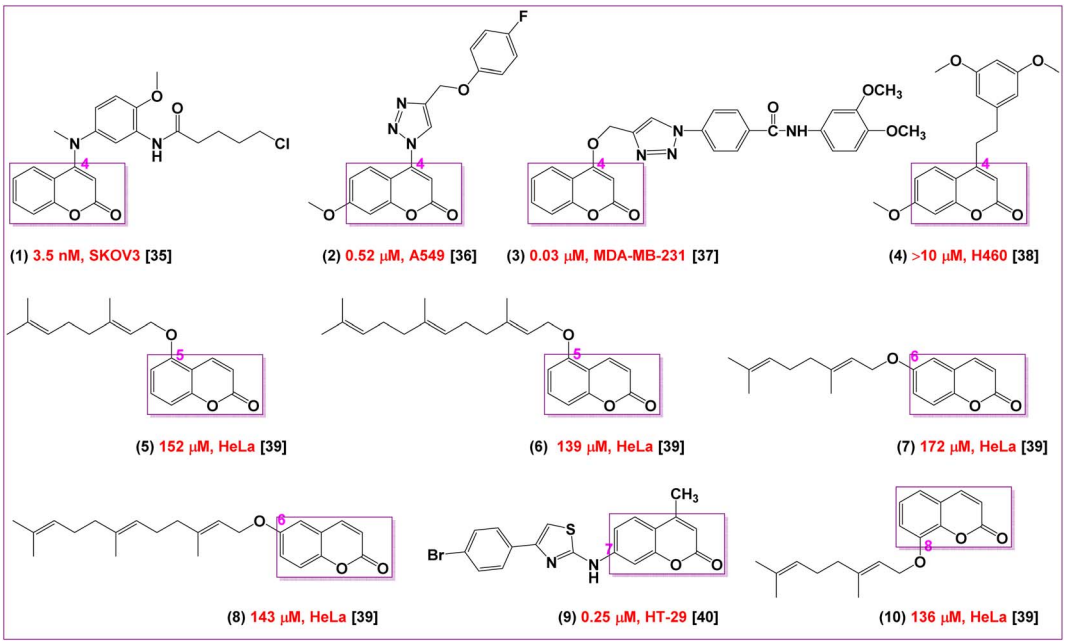

Fig. 1 The basic structural substitution requirements for coumarin moiety as reported.

pharmacophoric features that has crucial role to form hydrogen bonding acceptors and donors as a naturally present in the human body. These hybrid chemical modifications are hopefully expected to improve their cytotoxic activities and therefore reduce their side effects.

Therefore, the main core of rational design encompasses the following bioisosteric chemical features which include; coumarin moiety, amide linker at the 7-position of coumarin nucleus, connected with phenyl ring, aliphatic moiety, or hydrophilic moiety (Fig. 2). Thus, the rational drug design generates new target hybrid structures with different biological isosteres with the hope that these new hybrid compounds might lead to a potential safe, effective, and potent as anticancer activity.

2 Results and discussion

2.1. Chemistry

The synthesis of target compounds **5a–c**, **7a–c** and **9a–c** were presented in Scheme 1 and 2. Firstly, the key starting intermediate compound **2** was synthesized according to the most extensively applied method, Pechmann condensation reaction of coumarin synthesis,[52,53] by stirring a mixture of activated resorcinol **1** and ethyl acetoacetate in the presence of Conc. H_2SO_4 as a catalyst under solvent-free conditions for 18 h to obtain corresponding 7-hydroxy-4-methyl-2*H*-chromen-2-one (**2**). Then compound **2** was allowed to react with ethyl chloroacetate (β-ketoester) in the presence of dry acetone and anhydrous potassium carbonate to give ester derivative, compound **3**. The corresponding acid hydrazide derivative **4** can be synthesized by the reaction of compound **3** with hydrazine hydrate in the presence of ethanol. The target peptide derivatives **5a–c** was prepared by a coupling reaction of compound **4** with appropriate amino acids, *via* azide-coupling method[54] in good yields (Scheme 1). The hydrazide is converted to acyl azide in the presence of HNO_2. Then amino acid esters were introduced which reacts with the acyl azide to form an amide bond, which typically takes several hours. Low temperature is required to prevent decomposition of azide which releases nitrogen gas. Furthermore, the coupling step is achieved under basic a condition which prevents the formation of hydrazoic acid (HN_3). The structures of the newly synthesized compounds **5a–c** were established on the basis of elemental analysis and spectral data.

Treatment of the peptide derivative, compounds **5a** and **7a** with excess hydrazine hydrate in ethanol afforded the corresponding hydrazide **6** and **8** in a good yield, respectively. The dipeptides **7a–c** and tri-peptides **9a–c** were successfully obtained in very good yields from compounds **6** and **8**, respectively by similar general methodology mentioned in the synthesis of mono-peptides **5a–c** under the same condition (Scheme 2). The chemical structures of these set of novel compounds **7a–c** and **9a–c** were established by their spectral and elemental analyses.

2.2. Biological evaluation

2.2.1 ***In vitro*** **anticancer screening.** The new synthesized compounds were initially evaluated for their *in vitro* antiproliferative activities against three different cancer cell lines, namely hepatocellular carcinoma (HepG-2), prostate carcinoma (PC-3), and colorectal carcinoma (HCT-116). The antiproliferative activities were performed using doxorubicin as a positive control and determined *via* MTT assay techniques.[55]

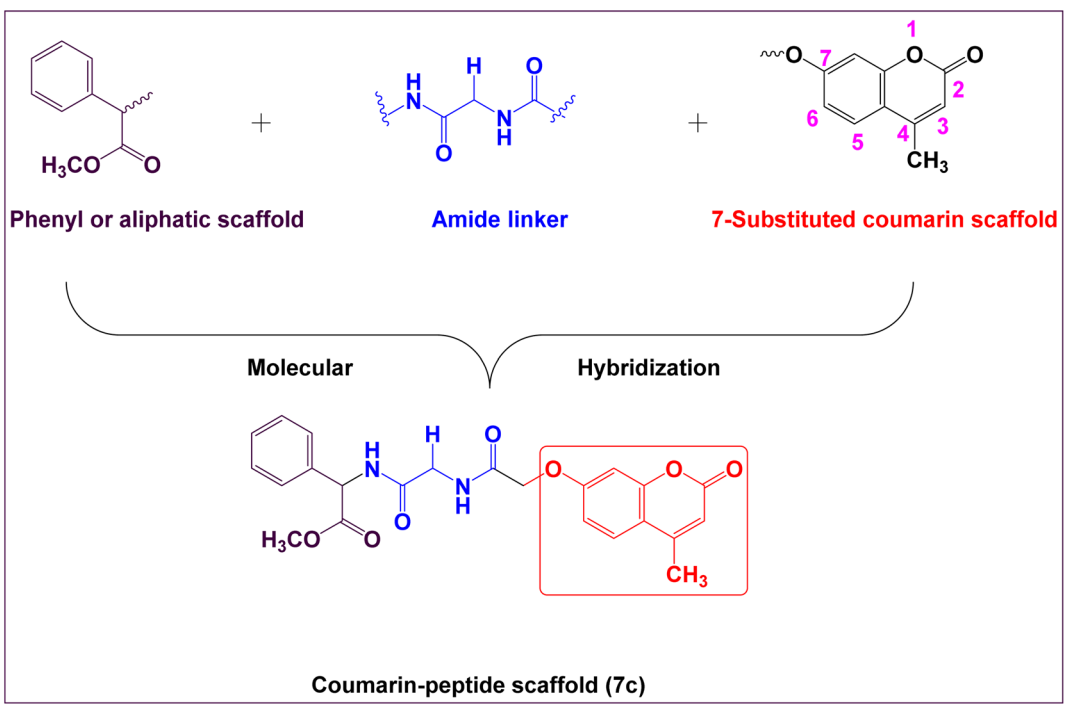

Fig. 2 Planned design of novel coumarin derivatives for antitumor activity.

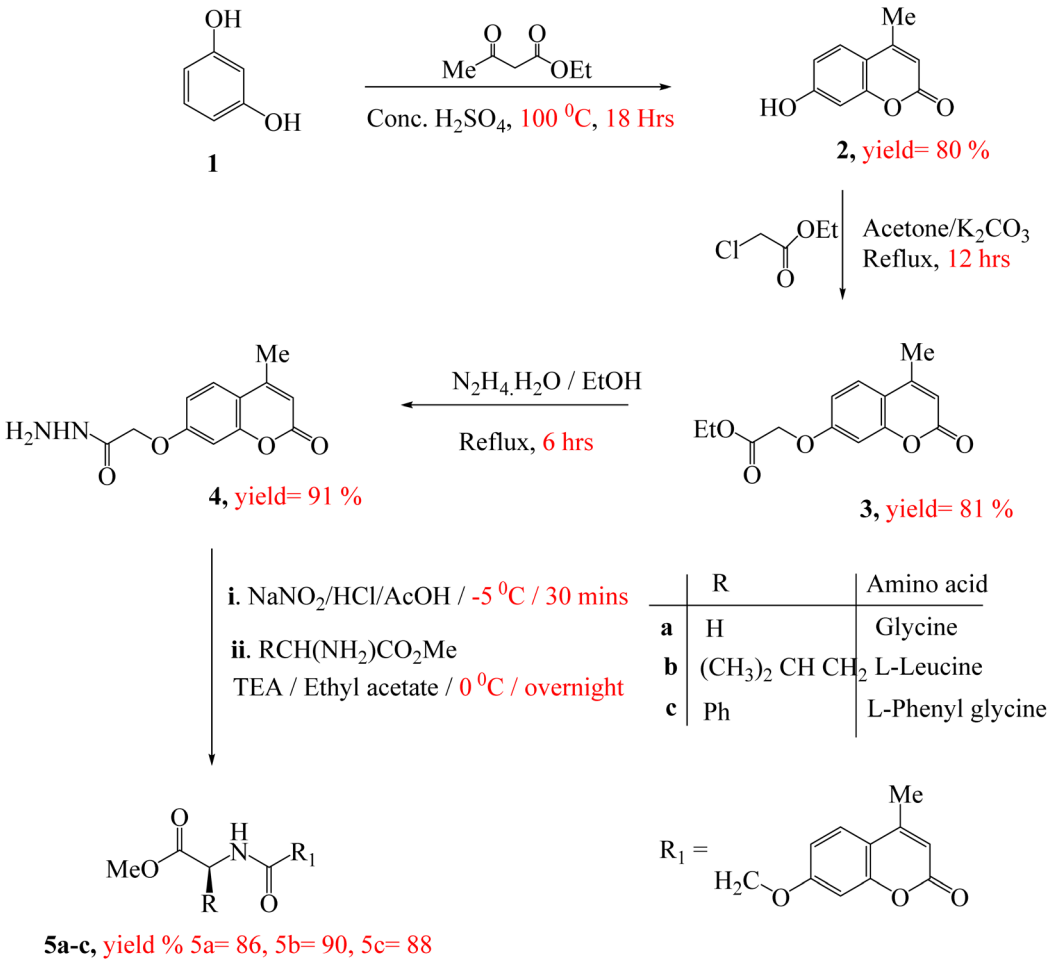

Scheme 1 Synthetic route of target compounds 5a–c.

The obtained results of anticancer activities indicated that the screened chemical compounds showed obviously different levels of cytotoxic activity ranging from potent, moderate, and weak cytotoxicity in the treatment of all tested tumor cell lines. Therefore, data represented in (Table 1) revealed that, compound **7c** distinctly appeared to be the most potent cytotoxic candidate, and efficient than doxorubicin with IC_{50} values of 34.07, 16.06, and 16.02 μM against three human cancer cell lines (HepG-2, PC-3, and HCT-116) indicating broad-spectrum anticancer activity. These results displayed that the hybrid structure possesses di-peptide linker with coumarin nucleus and substituted at the 7-position with mainly aromatic ring was more potent than those possessing mono-peptide and tri-peptide linkers substituted with aliphatic group **5b**, **7b**, **5a** leading to a significant decrease in cytotoxic activity.

Moreover, compound **5b**, substituted with aliphatic moiety appeared to be the most potent derivative against three cell lines with IC_{50} values of 42.16, 59.74, and 35.05 μM in comparison to an anticancer drug, doxorubicin as standard drug. Besides, compounds **7b**, and **5a** possessed excellent anti-proliferative activities against three tested cell lines with IC_{50} values ranging from 61.01 μM to 105.74 μM indicating that the number of peptide bond can affect the anticancer property and gave the highest activity with the most potent compound with di-peptide bond, **7c**.

Furthermore, several analogs such as **8**, **5c**, **6**, and **7a** demonstrated moderate anti-proliferative activities with IC_{50} values ranging from 63.74 μM to 173.89 μM, which probably due to the fact that incorporation of a hydrophilic group leading to unfavorable interaction with target receptor.

Finally, various compounds **9a**, **9b**, and **9c**, exhibited relatively weak cytotoxicity towards three cell lines, indicating that the tri-peptide moiety did not play a key role in increasing their anti-cancer activities.

2.2.2 CK2 kinase enzyme inhibitory assay. Based on the rational design of the target compounds, a series of active amino acid derivatives linked to coumarin moiety was designed according to the bioisosteric chemical modification and chemically synthesized by usual technique. The antitumor activities of the new synthesized compounds were investigated biologically for their cytotoxic activities against three different cancer cell lines, belonging to different tumor types. The target compounds have promising antitumor activity and proposed as CK2 inhibitors.[56–58] Thus, the most potent active compounds with excellent anti-proliferative activities were further selected and evaluated for their activities against CK2 inhibitors

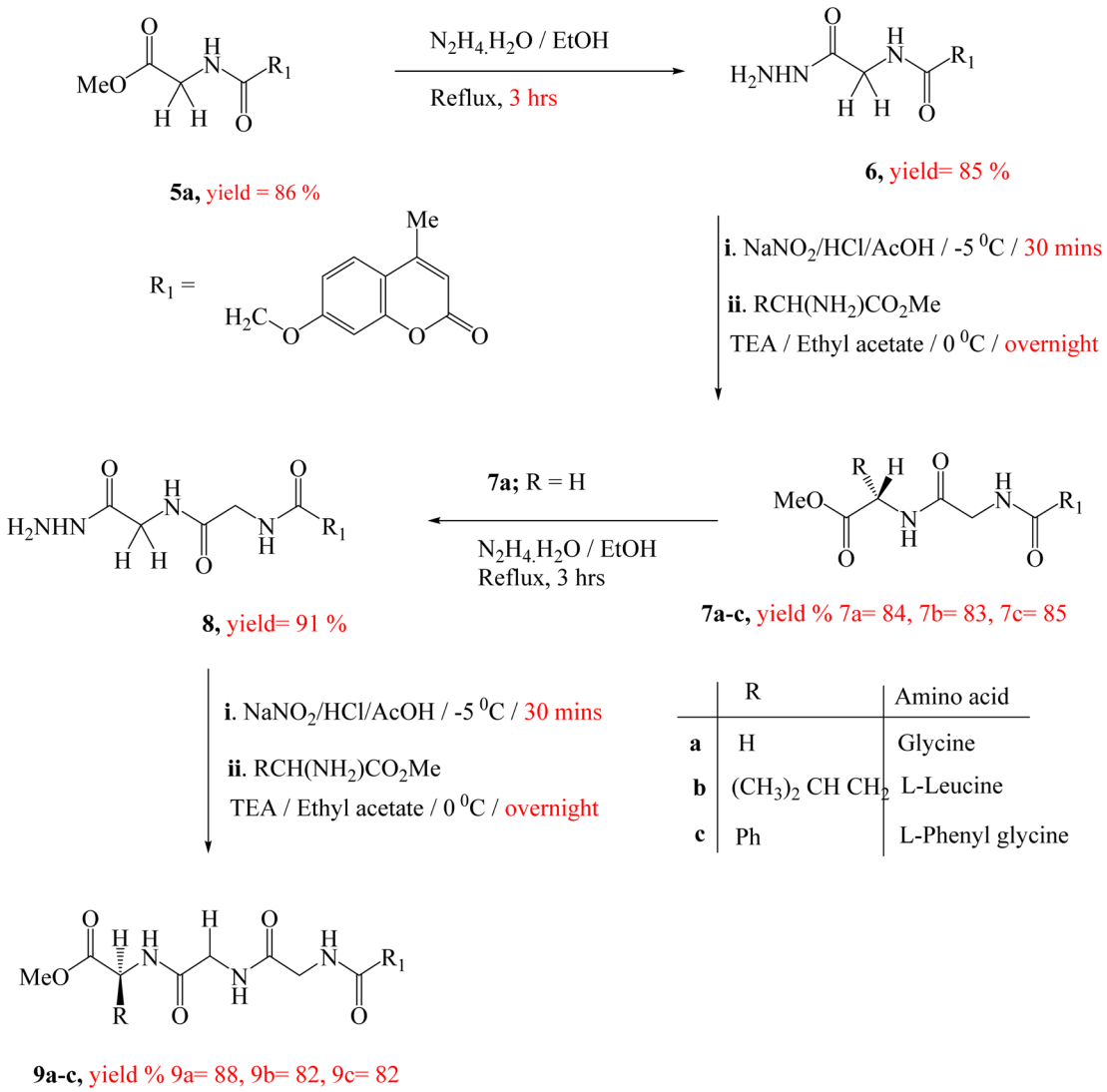

	R	Amino acid
a	H	Glycine
b	$(CH_3)_2$ CH CH_2	L-Leucine
c	Ph	L-Phenyl glycine

Scheme 2 Synthetic route of target compounds 7a–c & 9a–c.

according to (ref. 59). Roscovetine as one of the most potent CK2 inhibitors was used as a positive control.[60] The most potent compound **5b** exhibited excellent inhibition against CK2 kinase with IC_{50} value of 0.117 ± 0.005 μM compared with roscovetine as control drug with IC_{50} value of 0.251 ± 0.011 μM (Table 2). However, compound **7c** incorporating a phenyl moiety, appeared to be less active against CK2 kinase (Fig. 3).

2.2.3 Molecular docking. Protein kinase 2 (CK2), previously known as casein kinase 2, is considered an interesting potential therapeutic target for cancer therapy.[61,62] In addition, the binding site of CK2 has been reported as potent and selective CK2 for cancer treatment using coumarin derivatives.[49–51] To better comprehend how synthesized compounds contributed to CK2 inhibitory activities, molecular docking investigations were conducted by using AutoDock 4.2 program. The synthesized compounds were docked to the active site of CK2 co-crystallized with **G12** (PDB ID: 2QC6). The molecular docking results show that the binding site location of redocked **G12** was roughly the same as that of co-crystallized ligand. Moreover, all synthesized compounds were bound to the active site of CK2, and the binding modes were similar to that of reference ligand.

The obtained binding mode of co-crystalized ligand, **G12** revealed that the hydroxyl group at the 7-position was involved in a hydrogen bonding interaction with Lys68 and formed water-mediated interactions with Glu81 and backbone amino group of Asp175. The chromene core of co-crystalized ligand was also stabilized by an aromatic stacking interaction with Phe113 and located in the hydrophobic pocket formed by primarily with Val45, Val53, Ile66, Val95, Val116, Met163, and Ile174.

Compound **7c** as a representative example demonstrated a binding mode like that of co-crystalized ligand, **G12**, with multiple hydrophilic and hydrophobic interactions was found to facilitate the binding interactions of this compound to CK2 binding site. The carbonyl group at the 2-position was involved in the hydrogen bonding interaction with Lys68. And the oxygen atom at the 7-position of chromene nucleus was formed a water-mediated interaction with Asn118, with a water molecule that is

Table 1 *In vitro* cytotoxicity against hepatocellular carcinoma (HepG-2), prostate carcinoma (PC-3), and human colon cancer (HCT-116) activity of new synthesized compounds

	In vitro cytotoxicity[a] IC_{50} (μM)		
Compound no.	HePG2	PC-3	HCT-116
Doxorubicin	108 ± 0.6	57.34 ± 0.6	61.01 ± 0.3
5a	101.18 ± 0.3	105.74 ± 5.3	63.81 ± 3.6
5b	42.16 ± 0.3	59.74 ± 4.2	35.05 ± 2.8
5c	153.79 ± 2.1	173.89 ± 1.8	124.06 ± 4.4
6	168.32 ± 4.4	168.35 ± 4.3	171.34 ± 4.2
7a	173.82 ± 3.4	172.27 ± 1.4	137.45 ± 2.4
7b	72.13 ± 3.7	70.82 ± 2.1	61.01 ± 2.7
7c	34.07 ± 4.2	16.06 ± 4.6	16.02 ± 4.1
8	172.24 ± 4.3	63.74 ± 4.3	94.74 ± 4.0
9a	377.48 ± 2.5	115.01 ± 1.6	219.12 ± 2.8
9b	298.76 ± 0.3	85.5 ± 0.4	169.13 ± 0.3
9c	221.0 ± 0.9	147.29 ± 0.4	139.94 ± 0.7

[a] IC_{50} values are the mean ± standard deviation (SD) of three separate experiments.

Table 2 *In vitro* enzymatic inhibitory activities of the most potent target amino acid derivatives against CK2 kinase

Compound no.		Results
	MW g mol^{-1}	[a]IC_{50} μM
5b	361.39	0.117 ± 0.005
7c	438.43	0.461 ± 0.02
Roscovetine	354.5	0.251 ± 0.011

[a] IC_{50} values are the mean ± standard deviation (SD) of three separate experiments.

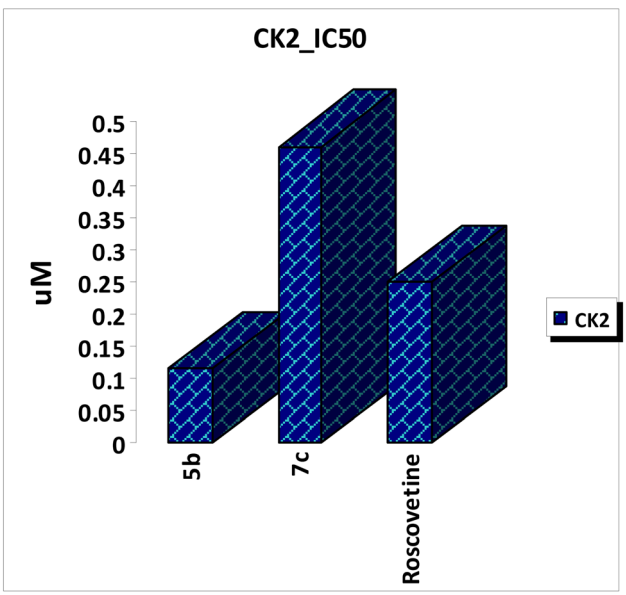

Fig. 3 *In vitro* enzymatic inhibitory activities of the most potent amino acid derivatives against CK2 kinase.

conserved in all deposited CK2 structure. The methyl group at the 4-position was stabilized by hydrophobic interactions with Ile66, Val95 and Phe113. Furthermore, the two amino groups of acetamido moieties were located in hydrophilic interactions with the carbonyl backbone of His60 and formed a water-mediated interaction with Val45. Chromene moiety was also stabilized by an aromatic stacking interaction with Phe113 and located in the hydrophobic pocket formed by Val45, Val116, Met163, and Ile174. The carbonyl group of acetate moiety was located in a hydrogen bonding interaction with backbone amino group of Arg47 as well as the phenyl ring was stabilized by cationic π interactions with Arg47 and Lys158, which enhancing the affinity of compound **7c** towards CK2 binding site (Fig. 4).

The binding mode of compound **5b** was like that of co-crystalized ligand and compound **7c**. The amino group of acetamide moiety was involved in a hydrogen bonding interaction with backbone carbonyl group of Val45 and the other carbonyl group of acetamide moiety was formed a water-mediated interaction with His160 and these network interactions with water molecule seems to have a crucial role in the recognition process. The hydrophobic leucinate group was located in an unfavorable hydrophilic interaction with Arg47, which may explain its lower affinity of compound **5b** compared with compound **7c** (Fig. 5).

The binding mode of compound **7b** (Fig. 6) was similar to compound **7c** that can completely accommodate the binding site. In addition, the hydrophobic glycylleucinate was located in an unfavorable hydrophilic interaction with Arg47. The molecular docking study results with protein kinase 2 receptor indicated that co-crystalized ligand, reference drug and synthesized compounds have similar binding mode patterns (Fig. 7) and our study has confirmed that most of the synthesized compounds have good binding affinities towards the receptor target ranging from −7.61 to −10.15 kcal mol^{-1}. Furthermore, the computed values of free energy of binding of the synthesized compounds reflect the overall trend (Table 3).

Analyzing the favorable binding pose, five different hydrogen bonding interactions were found, including, side-chains and backbones, Val45, Arg47, Lys68, Asn118 and His160 residues. In addition, higher hydrophobic contributions were found, due to a more deeply located binding pose inside the binding site of protein kinase 2 receptor. The mainly hydrophobic amino acid residues seem to be responsible for the affinity and selectivity of protein kinase 2 receptor, in particular, the interactions with Val45, Val53, Ile66, Val95, Phe113, Val116, Met163, and Ile174 could be responsible for the selectivity of protein kinase 2 receptor ligands and play an important role in protein kinase 2 inhibition which indicates the hydrophobic CK2 ATP-binding pocket. These fingerprints of interaction features can be used to improve and design new chemical compounds to yield better amino acid derivatives attached to coumarin nucleus in the search for the anticancer agents.

2.2.4 ADME/toxicity properties prediction. Many drugs still being characterized by high systemic toxicity mainly due to the lack of tumor selectivity and present pharmacokinetic adverse effects that are associated with low solubility, that negatively

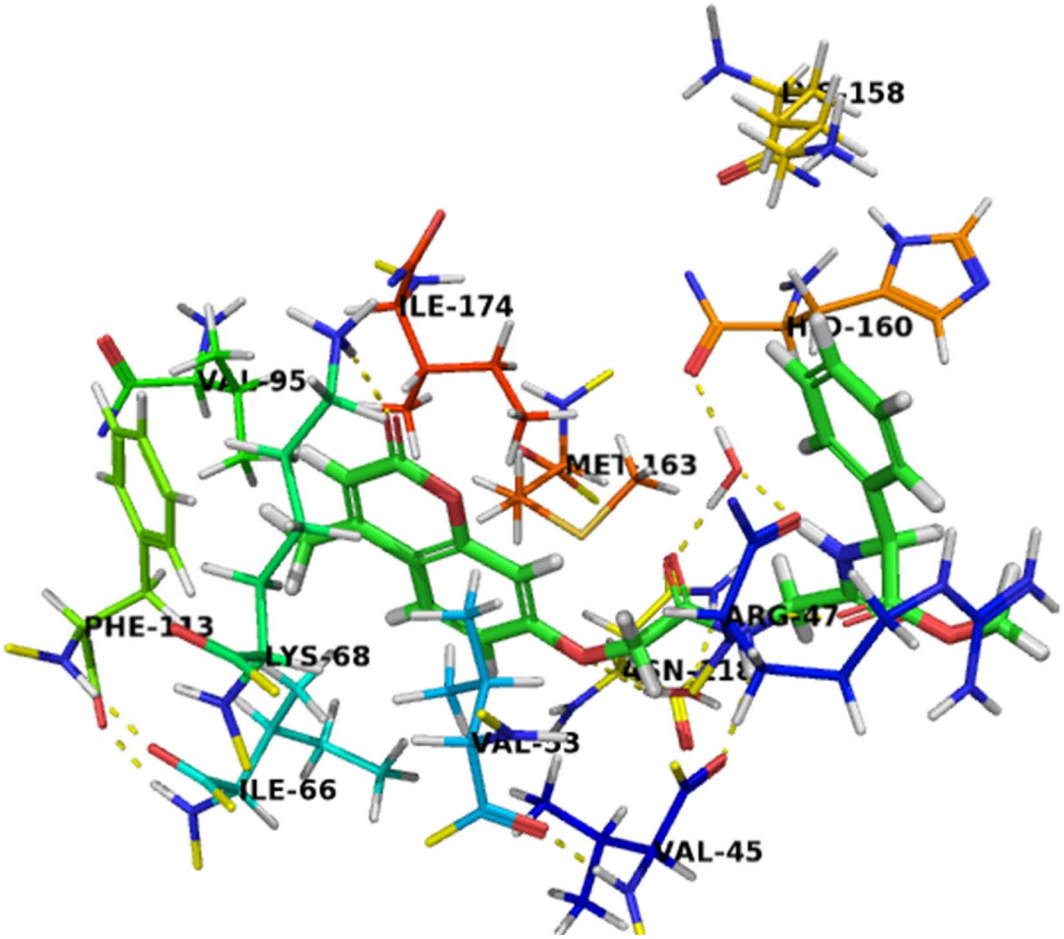

Fig. 4 Crystal structure of CK2 receptor (PDB ID: 2QC6) with compound **7c**. The hydrogen bonding interactions are presented by dashed lines. Residues contacting ligand are demonstrated as lines.

affect the drug circulation time and bioavailability.[63] Thus, we investigated considerable chemical descriptors and pharmacokinetic parameters relevant properties of the synthesized new compounds using QikProp (Schrodinger LLC) to predict chemical features and ADME descriptors.[64]

Among which were molecular weight, hydrogen bond-donors, hydrogen bond-acceptors, log *P*, log *p* MDCK according to Lipinski's rule of five[65] that characterizes molecular properties which are climacteric for drug's pharmacokinetics in the human body including its ADME parameter.

The partition coefficient (QPlogPo/w) and aqueous solubility (QPlogS), are critical for estimating the absorption, transport and distribution in the body. The absorption and distribution levels (QPlog(o/w)) of all synthesized compounds were ranged between 1.005 to 2.685 and −0.504 to −1.257 respectively. As a result, all synthesized compounds appeared to be good range.

Furthermore, the levels of cell permeability (QPPCaCO-2) and QPPMDCK, key factors governing drug metabolism and its access to biological membranes were ranged from 25.835 to 213.401 and 35.052 to 187.87 respectively. Thus, all the synthesized compounds have good cell permeability except compounds **7a**, **9a**, **9b**, and **9c** were predicted to get poor cell permeability.

In addition, the levels of (QPlogBB) penetration of the most compounds were expected to be safe to CNS, while compounds **9a**, **9b**, and **9c** were expected to have moderate (QPlogBB) penetration. Furthermore, the new synthesized compounds have favorable ADME properties and the percentage human oral absorption was predicted to be more than 81.47% and 62.284 for all biologically potent compounds (**5b** and **7b**). Therefore, all these pharmacokinetic parameters were within the acceptable range that defined for human use especially for active compounds, thereby indicating their potentials as drug-like molecules (Table 1, and ESI data†).

2.2.5 Structure–activity relationship (SAR). We aimed to investigate the SAR of newly synthesized compounds as potential anticancer activities, as summarized in the rationale drug design. SAR correlations were identified by examining the obtained results of biological data.

Therefore, structure activity relationship containing pharmacophoric features that are essential for explanation of their cytotoxic effects can be explained by a compound having a substitution at the 7-position of coumarin scaffold substituted with lengthy linker containing an aromatic amino acid (**7c**) was more potent than those possessing short linker (**5b**), or lengthy linker containing an aliphatic amino acid (**7b**), leading to

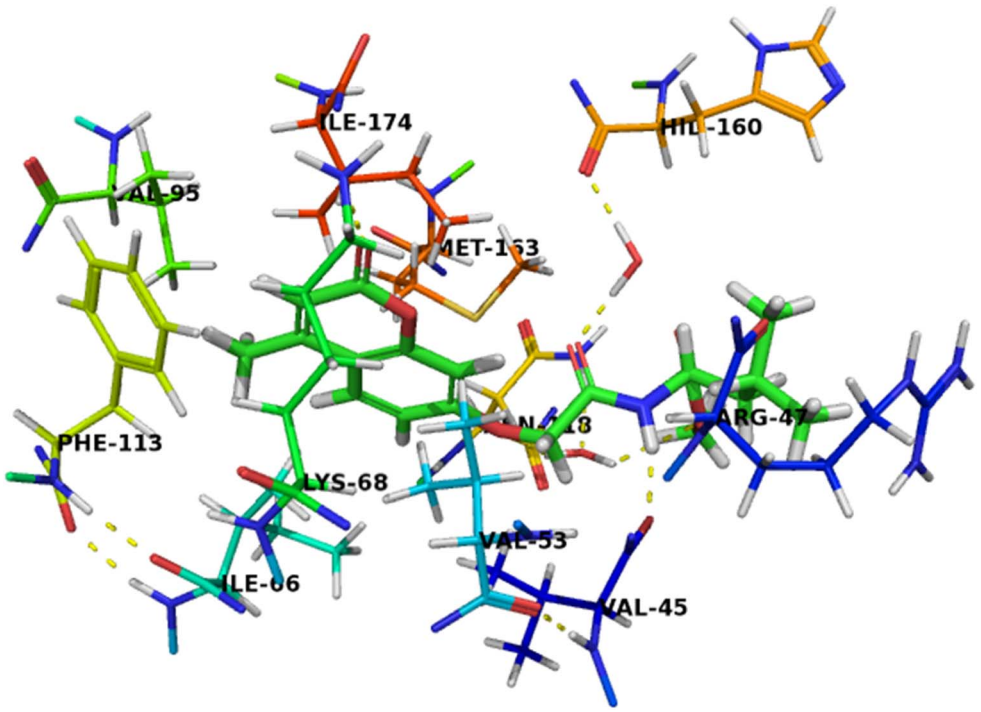

Fig. 5 Crystal structure of CK2 receptor (PDB ID: 2QC6) with compound **5b**. The hydrogen bonding interactions are presented by dashed lines. Residues contacting ligand are demonstrated as lines.

a significant decrease in cytotoxic activity and indicated that the substitution with lengthy aromatic amino acid linker is more preferred biologically. These results are in accordance with coumarin–amino acid generated by Naik *et al.* and Sousa *et al.* which indicated that conjugation with aromatic amino acids showed potent inhibition whereas aliphatic amino acids showed compelling inhibition.[66,67]

Moreover, the key structural features of amino acid indicated that di-peptide (**7c**) was more potent than those possessing mono-peptide and tri-peptide linkers leading to a significant decrease in cytotoxic activities (**5b**, **9a–c**) indicating that the number of peptide bond can affect the anticancer property and gave the highest activity with the most potent compound with di-peptide bond, (**7c**).[68] On the other hand,[69,70] the incorporation of a hydrophilic group seems to be a contributing factor for decreasing antitumor activity (**6**, **8**) (Fig. 8).

3 Experimental

3.1. Chemistry

All the chemical compounds which employed in this study were commercially available with analytical grade and used without any further purification. Solvents were purified and freshly distilled before using according to the standard procedures. The progress of the reaction mixtures was monitored by thin layer chromatography (TLC). The spots on the TLC plates were visualized with a UV lamp (254 nm). Melting points were measured using Thermo Fisher Scientific. IR spectra were recorded Bruker tensor 27, FT-IR Spectrophotometer. All ^{1}H NMR and ^{13}C NMR spectra were recorded on a Bruker 400 and 100 MHz Spectrophotometer. Chemical shifts (δ) are reported in parts per million (ppm) using tetramethylsilane (TMS) as an internal standard. Ultraviolet-visible (UV-vis) absorption spectra were recorded on PerkinElmer spectrophotometer at the wavelength of maximum absorption (k_{max}) in a range of DMSO at same concentrations (1×10^{-6} M). The mass spectra were run on a Shimadzu QP 5050 Ex Spectrometer. The microanalyses for C, H and N were performed on PerkinElmer elemental analyzer. All compounds were within $\pm$0.4 of the theoretical values.

3.1.1 Synthesis of 7-hydroxy-4-methyl-2*H*-chromen-2-one (2).[58] To a stirred mixture of resorcinol (0.1 mole, 11 g) and ethyl acetoacetate (0.1 mole, 13 g) a concentered sulphuric acid (0.1 mole, 9.8 ml) was added drop-wise at room temperature, then heat these mixture at 100 °C with occasional stirring for 18 h. The mixture was poured into crushed ice-water. The precipitated was filter off, washes with cold water and recrystallized from aqueous alcohol to give compound **2**, yield: 14.08 g (80.0%); mp 188–190 °C [lit. yield 81–82%; mp 190–192 °C].[71]

3.1.2 Synthesis of ethyl-2-[(4-methyl-2-oxo-2*H*-chromen-7-yl)-oxy]acetate (3).[58] A mixture of 7-hydroxy-4-methylchromen-2-one, **2** (0.01 mole, 1.76 g), ethyl chloroacetate (0.01 mole, 1.22 ml) and anhydrous potassium carbonate (0.01 mole, 1.38 g) in dry acetone was refluxed for about 12 h. The mixture was filtered on heat then poured into cold ice-water. Filtrate and the resulting solid substance was washed with excess of water. The crude product was purified by crystallization from ethanol to afford compound, **3**; yield: 1.42 g, (81%), mp 92–94 °C [lit. yield 81–2%; 94–96 °C]. IR ν:(KBr, cm^{-1}): 3069 (CH aromatic), 2979 (CH aliphatic), 1714 (C=O ester), 1612 (C=C).

3.1.3 General procedure for synthesis of hydrazide derivatives 4, 6 and 8. A mixture of ethyl-2-[(4-methyl-2-oxo-2*H*-

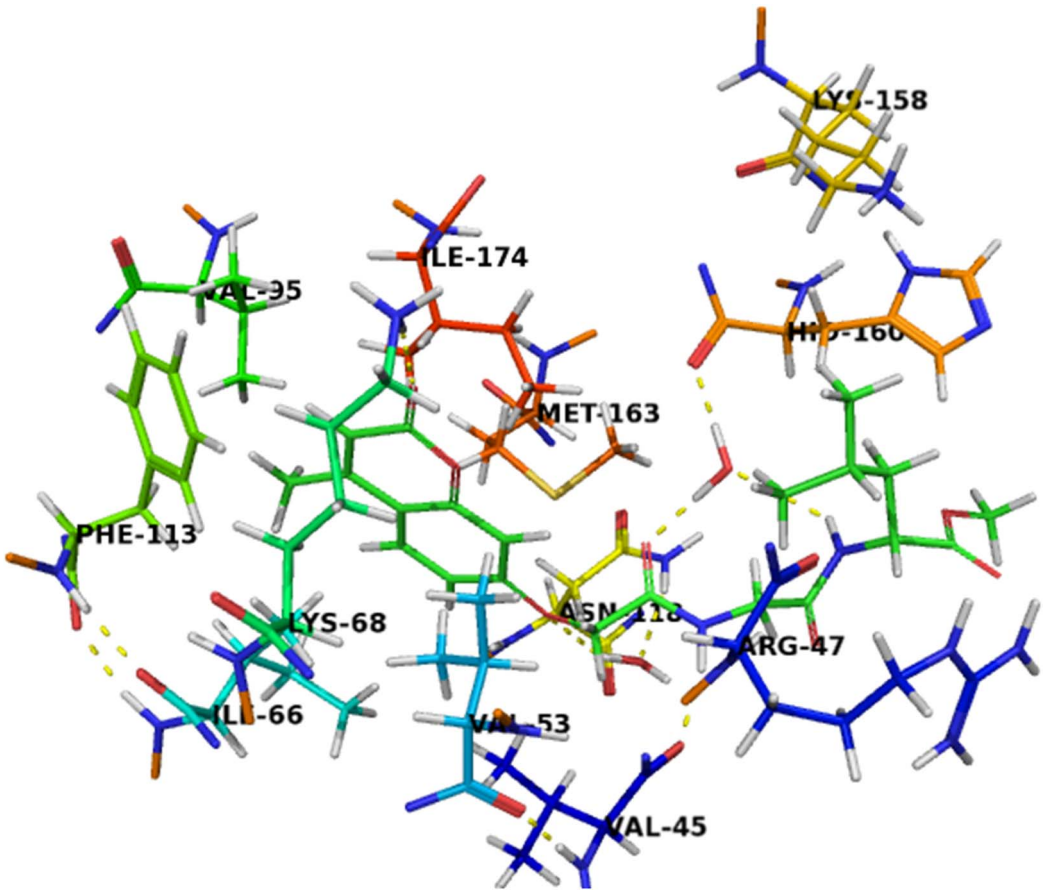

Fig. 6 Crystal structure of CK2 receptor (PDB ID: 2QC6) with compound **7b**. The hydrogen bonding interactions are presented by dashed lines. Residues contacting ligand are demonstrated as lines.

chromen-7-yl)-oxy] acetate (**3**), methyl 2-{2-[(4-methyl-2-oxo-2*H*-chromen-7-yl)oxy]acetamido}acetate (**5a**) and methyl 2-{2-[2-[(4-methyl-2-oxo-2*H*-chromen-7-yl)oxy]acetamido]acetamido} acetate (**7a**) (0.01 mole), respectively and hydrazine hydrate 99% (0.01 mole) in absolute ethanol (20 ml) was heated under reflux for 3–6 h. The excess of ethanol was removed under reduced pressure and the resulting precipitate was filtered off and recrystallized from appropriate solvent to give compounds **4**, **6**, and **8**, respectively in good yields.

3.1.4 2-[(4-Methyl-2-oxo-2*H*-chromen-7-yl)-oxy] acetohydrazide (4).[58] A needle crystals, mp 194–196 °C ($CHCl_3$/MeOH) [lit. 200–204 °C]; yield: 87%; IR ν:(KBr, cm^{-1}): 3423, 3329 (NH_2), 33 266 (NH), 3079 (CH aromatic), 2978 (CH aliphatic), 1675 (C=O, amide), 1610 (C=C), 1509 (C–N).

3.1.5 *N*-(2-Hydrazinyl-2-oxoethyl)-2-[(4-methyl-2-oxo-2*H*-chromen-7-yl)oxy]acetamide (6). Yellowish white crystal, mp 162–164 °C (ethanol); yield: (85%); $R_f = 0.48$ (2% MeOH/$CHCl_3$); IR ν:(KBr, cm^{-1}): 3735 (NH_2), 3291 (NH), 3059 (CH aromatic), 2917 (CH aliphatic), 1713 (C=O, lactone), 1660 (C=O, amide), 1614 (C=C), 1548 (C–N).

3.1.6 *N*-(2-Hydrazinyl-2-oxoethyl)-2-{2-[(4-methyl-2-oxo-2*H*-chromen-7yl)oxy]acetamido} acetamide (8). Yellowish white crystals, mp 158–160 °C (ethanol); yield: (91%); $R_f = 0.45$ (2% MeOH/$CHCl_3$); IR ν:(KBr, cm^{-1}): 3831, 3754 (NH_2), 3282 (NH), 3085 (CH aromatic), 2924 (CH aliphatic), 1661 (C=O, amide), 1611 (C=C), 1550 (C–N).

3.1.7 General procedure for synthesis of 2-[(4-methyl-2-oxo-2*H*-chromen-7-yl)oxy]aceto bearing amino acid esters 5a–c, 7a–c and 9a–c. A solution of a corresponding hydrazides, **4**, **6**, and **8** (4 mmol), respectively in acetic acid (30 ml), 1 N HCl (15 ml), and water (125 ml) was cooled in an ice-bath (−5 °C). Sodium nitrite (4.35 g, 63 mmol) in cold water (15 ml) was added with stirring. After stirring at −5 °C for 15 min, a yellow syrup of azide was formed, which was taken up in cold ethyl acetate (150 ml), washed with $NaHCO_3$ (3%, 150 ml) and water (150 ml), and dried over Na_2SO_4. A solution of the corresponding amino acid methyl ester hydrochloride (4.5 mmol) in ethyl acetate (100 ml) containing triethyl amine (1.0 ml) was stirred at 0 °C for 20 min and filtered, and the filtrate was added to the azide solution. The mixture was kept at −5 °C for 12 h, then at room temperature for another 12 h, followed by washing with 0.5 N HC1 (150 ml), 3% $NaHCO_3$ (150 ml), and water (150 ml), and drying over Na_2SO_4. The filtrate was evaporated under reduced pressure, and the residue was purified by silica gel column chromatography (petroleum ether–ethyl acetate, 5 : 1) to afford the corresponding product **5a–c**, **7a–c** and **9a–c**.

3.1.8 Methyl 2-{2-[(4-methyl-2-oxo-2*H*-chromen-7-yl)oxy} acetamide]acetate (5a). A white crystals, yield (86%); mp 178–

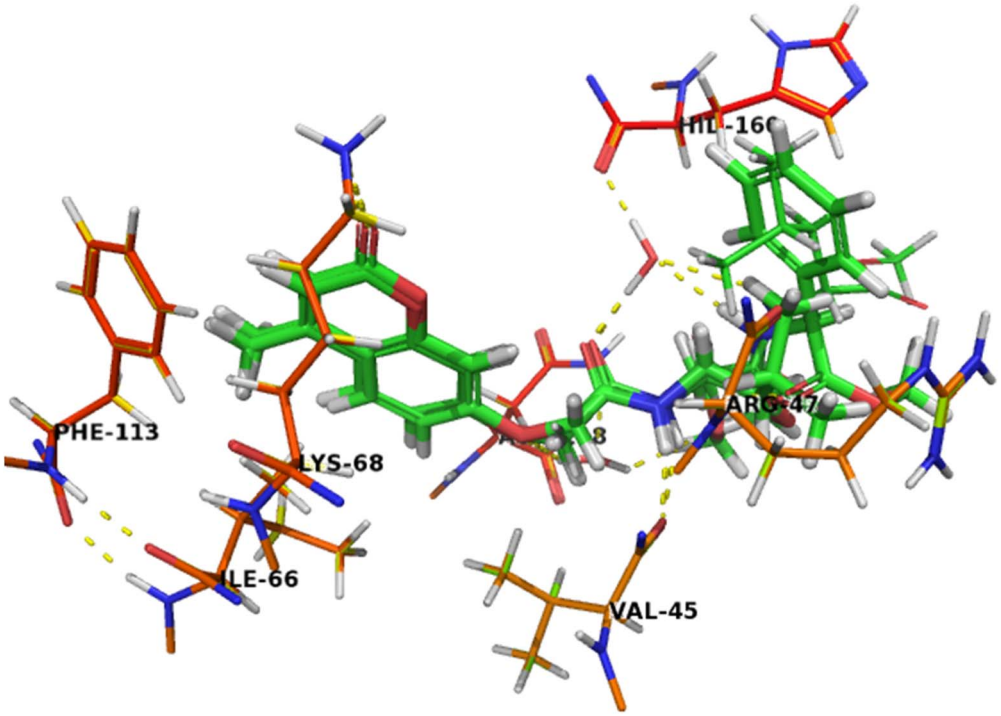

Fig. 7 Crystal structure of CK2 receptor (PDB ID: 2QC6) with aligned compounds, **7c**, **5b**, **7b** and **5a**. The hydrogen bonding interactions are presented by dashed lines. Residues contacting ligand are demonstrated as lines.

182 °C; R_f = 0.45 (2% MeOH/$CHCl_3$); IR ν:(KBr, cm^{-1}): 3372 (NH), 3075 (CH aromatic), 2923 (CH aliphatic), 1727 (C=O ester), 1673 (C=O amide), 1610 (C=C), 1507 (C–N); ^{1}H NMR (400 MHz; DMSO-d_6) δ (ppm): 2.41 (s, 3H, H_4–CH_3); 3.65 (s, 3H, O–CH_3); 3.92–3.94 (d, 2H, J = 8 Hz, (C=O)CH_2NH); 4.70 (s, 2H, O–CH_2(C=O); 6.24 (s, 1H, H-3 coumarin)); 6.98 (d, 1H, J = 2.8 Hz, H-8 coumarin); 7.01–7.04 (dd, 1H, J = 8.8 Hz 2.8 Hz, H-6 coumarin), 7.71–7.73 (d, 1H, J = 8.8 Hz, H-5 coumarin) 8.64 (t,

Table 3 Summary of free energy of binding, hydrophilic and hydrophobic interactions, and hydrogen bonding interactions of coumarin derivatives with CK2 binding site

Comp. no.	Total energy (kcal mol^{-1})	Hydrophilic and hydrophobic interactions	Hydrogen bonding interactions
5a	−8.20	Val45, Val53, Ile66, Val95, Phe113, Val116, Met163, and Ile174	Arg47, Lys68, Asn118, and His160
5b	−8.28	Val45, Val53, Ile66, Val95, Phe113, Val116, Met163, and Ile174	Val45, Arg47, Lys68, Asn118 and His160
5c	−7.68	Val45, Arg47, Val53, Ile66, Val95, Phe113, Val116, Phe121, Met163, and Ile174	Val45, Lys68, Asn118, His160, and Asp175
6	−8.43	Val45, Val53, Ile66, Val95, Phe113, Val116, Met163, Phe121, and Ile174	Val45, Lys68, Asn118, Asp120, Asp175, and His160
7a	−7.94	Val45, Val53, Ile66, Val95, Phe113, Val116, Met163, Phe121, and Ile174	Val45, Lys68, Asn118 and His160
7b	−8.24	Val45, Val53, Ile66, Val95, Phe113, Val116, Phe121, Met163, and Ile174	Val45, Arg47, Lys68, and Asn118
7c	−10.15	Val45, Val53, Ile66, Val95, Phe113, Val116, Met163, and Ile174	Val45, Arg47, Lys68, Asn118 and His160
8	−7.92	Val45, Val53, Ile66, Val95, Phe113, Phe121, Met163, and Ile174	Arg47, Lys68, Asn118, Asp120, and His160
9a	−7.61	Val45, Val53, Ile66, Val95, Phe113, Val116, Phe121, Met163, and Ile174	Val45, Arg47, Lys68, Asn118, and His160
9b	−7.79	Val45, Val53, Ile66, Val95, Phe113, Val116, Phe121, Met163, and Ile174	Val45, Lys68, Asn118, Asp120, and His160
9c	−7.82	Val45, Val53, Ile66, Val95, Phe113, Val116, Phe121, Met163, and Ile174	Val45, Lys68, Asn118 Asp120, and His160

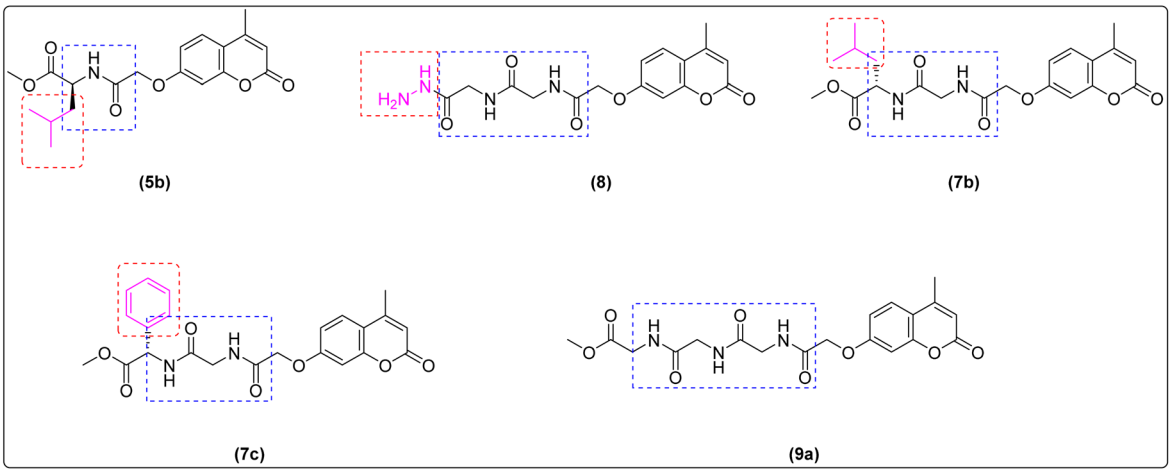

Fig. 8 SAR of newly synthesized compounds.

1H, J = 5.6 Hz, (C=O)CH_2NH); ^{13}C NMR (100 MHz; DMSO-d_6) δ (ppm): 18.6, 45.8, 52.2, 67.4, 102.2, 111.9, 113.0, 114.1, 126.9, 153.8, 154.9, 160.5, 161.0, 168.1, 170.4; MS (EI, 70 eV) m/z (%): 307 (M^+ + 2, 2.74), 306 (17.33), 305 (100), 297 (10.51), 246 (9.43), 217 (4.38), 189 (35.47), 178 (13.76), for $C_{15}H_{15}NO_6$ (305.28): calcd% C 59.01, H 4.95, N 4.59, O 31.45; found: % C 59.12, H 4.85, N 4.3.

3.1.9 (*S*)-Methyl-4-methyl-2-{2-[(4-methyl-2-oxo-2*H*-chromen-7-yl)oxy]acetamido}pentanoate (5b). A yellow oil, yield: (90%); R_f = 0.40 (2% MeOH/$CHCl_3$); IR ν:(KBr, cm^{-1}): 3432 (NH), 3060 (CH aromatic), 2990 (CH aliphatic), 1711 (C=O, ester), 1665 (C=O, amide), 1613 (C=C), 1507 (C–N); ^{1}H NMR (400 MHz; DMSO-d_6) δ (ppm): 1.08–1.12 (dd, 6H, J = 8, 16 Hz, $(CH_3)_2$ CH), 1.49 (m, 1H, $(CH_3)_2$ CH), 1.89 (m, 2H, CHCH_2CH), 2.35 (s, 3H, H_4–CH_3); 3.63 (s, 3H, O–CH_3); 4.41 (s, 2H, O–CH_2(C=O); 6.95 (s, 1H, H-3 coumarin)); 7.00 (s, 1H, H-8 coumarin); 7.02–7.05 (dd, 1H, J = 8.4 Hz, 2.4 Hz, H-6 coumarin), 7.70–7.73 (d, 1H, J = 12 Hz, H-5 coumarin) 8.30–8.32 (d, 1H, J = 8 Hz, (C=O)CHNH); 8.35 (t, 1H, J = 5.6 Hz, (C=O)CH_2NH); ^{13}C NMR (100 MHz; DMSO-d_6) δ (ppm): 18.6, 22.1, 45.5, 67.78, 101.6, 111.1, 113.0, 114.1, 126.9, 153.8, 154.9, 160.5, 161.0, 168.1, 170.4; MS (EI, 70 eV) m/z (%): 363 (M^+ + 2, 0.14), 362 (0.88), 361 (100), 305 (13.43), 234 (69.60), 205 (41.75), 189 (9.41), 176 (10.24), for $C_{19}H_{23}NO_6$ (361.39): calcd% C 63.15, H 6.41, N 3.88; found: % C 63.22, H 6.38, N 3.93.

3.1.10 (*S*)-Methyl 2-{2-[(4-methyl-2-oxo-2*H*-chromen-7-yl)oxy]acetamido}-2-phenylacetate (5c). A white foam, yield: (88%); mp 110–112 °C; R_f = 0.50 (2% MeOH/$CHCl_3$); IR ν:(KBr, cm^{-1}): 3338 (NH), 3083 (CH aromatic), 2946 (CH aliphatic), 1750 (C=O, ester), 1684 (C=O, amide), 1613 (C=C), 1531 (C–N); ^{1}H NMR (400 MHz; DMSO-d_6) δ (ppm): 2.40 (s, 3H, H_4–CH_3); 3.65 (s, 3H, O–CH_3); 4.77 (s, 2H, O–CH_2(C=O)); 5.50–5.52 (d, 1H, J = 8 Hz, (C=O)CHNH); 6.23 (s, 1H, H-3 coumarin); 6.94 (d, 1H, J = 2.8 Hz, H-8 coumarin); 6.97–7.00 (dd, 1H, J = 8.8 Hz 2.8 Hz, H-6 coumarin), 7.36–7.44 (m, 5H, Ar–H), 7.68–7.70 (d, 1H, J = 8.8 Hz, H-5 coumarin) 8.64 (d, 1H, J = 7.2 Hz, (C=O)CHNH); ^{13}C NMR (100 MHz; DMSO-d_6) δ (ppm): 18.6, 52.8, 56.5, 67.0, 101.9, 111.8, 112.9, 114.0, 126.9, 128.2, 128.8, 129.1, 136.4, 153.8, 154.9, 160.5, 161.3, 167.5, 171.1; MS (EI, 70 eV) m/z (%): 382 (M^+ + 1, 5.30), 381 (20.23), 323 (22.45), 322 (100), 189 (17.58), 176 (18.58), for $C_{21}H_{19}NO_6$ (381.38): calcd% C 66.13, H 5.04, N 3.67; found: % C 66.16, H 5.09, N 3.59.

3.1.11 Methyl 2-{2-[2-[(4-methyl-2-oxo-2*H*-chromen-7-yl)oxy]acetamido]acetamido}acetate (7a). A white crystals, yield: (84%); mp 198–201 °C; R_f = 0.38 (2% MeOH/$CHCl_3$); IR ν:(KBr, cm^{-1}): 3361, 329 (2NH), 3085 (CH aromatic), 2934 (CH aliphatic), 1729 (C=O, ester), 1664 (C=O, amide), 1622 (C=C), 1546 (C–N); ^{1}H NMR (400 MHz; DMSO-d_6) δ (ppm): 2.41 (s, 3H, H_4–CH_3); 3.63 (s, 3H, O–CH_3); 3.82–3.83 (d, 2H, J = 4 Hz, (C=O)CH_2NH); 3.86–3.88 (d, 2H, J = 4 Hz, (C=O)CH_2NH); 4.68 (s, 2H, O–CH_2(C=O); 6.24 (s, 1H, H-3 coumarin)); 7.01 (s, 1H, H-8 coumarin); 7.02–7.05 (dd, 1H, J = 8.4 Hz 2.4 Hz, H-6 coumarin), 7.71–7.74 (d, 1H, J = 12 Hz, H-5 coumarin) 8.37 (t, 1H, J = 8 Hz, (C=O)CH_2NH); 8.45 (t, 1H, J = 8 Hz, (C=O)CH_2NH); ^{13}C NMR (100 MHz; DMSO-d_6) δ (ppm): 18.6, 41.0, 41.9, 52.1, 67.5, 102.1, 111.9, 112.9, 114.1, 127.0, 153.8, 155.0, 160.5, 161.0, 167.8, 169.5, 170.6; MS (EI, 70 eV) m/z (%): 364 (M^+ + 2, 1.84), 362 (44.69), 330 (18.70), 274 (31.03), 246 (18.63), 187 (100), 177 (30.98), 148.05 (20.22), for $C_{17}H_{18}N_2O_6$ (362.33): calcd% C 56.35, H 5.01, N 7.73; found: % C 56.45, H 5.08, N 7.78.

3.1.12 (*S*)-Methyl-4-methyl-2-{2-{2-[(4-methyl-2-oxo-2*H*-chromen7yl)oxy]acetamido}acetamido} pentanoate (7b). A white crystal; yield: (83%); mp 144–150 °C; R_f = 0.38 (2% MeOH/$CHCl_3$); IR ν:(KBr, cm^{-1}): 3438, 3367 (2NH), 3077 (CH aromatic), 2952 (CH aliphatic), 1714 (C=O, ester), 1672 (C=O, amide), 1625 (C=C), 1536 (C–N); ^{1}H NMR (400 MHz; DMSO-d_6) δ (ppm): 0.83–0.89 (dd, 6H, J = 6.4, 12 Hz, $(CH_3)_2$ CH), 1.49 (m, 1H, $(CH_3)_2$ CH), 1.63 (m, 2H, CHCH_2CH), 2.41 (s, 3H, H_4–CH_3); 3.63 (s, 3H, O–CH_3); 3.82–3.83 (d, 2H, J = 3.6 Hz, (C=O)CH_2NH); 3.86–3.88 (m, 2H, 2CHNH); 4.65 (s, 2H, O–CH_2(C=O); 6.95 (s, 1H, H-3 coumarin)); 7.00 (s, 1H, H-8 coumarin); 7.02–7.05 (dd, 1H, J = 8.4 Hz, 2.4 Hz, H-6 coumarin), 7.70–7.73 (d, 1H, J = 12 Hz, H-5 coumarin) 8.30–8.32 (d, 1H, J = 8 Hz, (C=O)CHNH); 8.35 (t, 1H, J = 5.6 Hz, (C=O)CH_2NH); ^{13}C NMR (100 MHz; DMSO-d_6) δ (ppm): 18.6, 21.7, 23.1, 24.6, 41.7, 46.0, 50.6, 52.3, 67.5, 102.1, 111.9, 112.9, 114.1, 127.0, 153.8, 155.0, 160.5, 161.1, 167.7, 169.0, 173.3; MS (EI, 70 eV) m/z (%): 419 (M^+ + 1, 1.60), 418 (6.26), 330 (15.15), 274 (7.64), 246 (12.97), 233 (39.07), 189

(32.41), 176 (33.91), 148 (57.14), 86 (100) for $C_{21}H_{26}N_2O_6$ (418.44): calcd% C 60.28, H 6.26, N 6.69; found: % C 60.34, H 6.29, N 6.75.

3.1.13 (*S*)-Methyl2-{2-{2-[(4-methyl-2-oxo-2*H*-chromen-7-yl) oxy]acetamido}acetamido}-2-phenylacetate (7c). A white crystals, yield: (85%); mp 170–172 °C $R_f = 0.55$ (2% MeOH/$CHCl_3$); IR ν:(KBr, cm^{-1}): 3437, 3366 (2NH), 3075 (CH aromatic), 2945 (CH aliphatic), 1715 (C=O, ester), 1671 (C=O, amide), 1627 (C=C), 1541 (C–N); ^{1}H NMR (400 MHz; DMSO-d_6) δ (ppm): 2.41 (s, 3H, H_4–CH_3); 3.60 (s, 3H, O–CH_3); 3.98–3.91 (d, 2H, J = 5.6 Hz, (C=O)CH_2NH); 4.68 (s, 2H, O–CH_2(C=O); 5.45–5.46 (d, 1H J = 702 Hz, Ph*CH*NH), 6.24 (s, 1H, H-3 coumarin)); 6.99 (s, 1H, H-8 coumarin); 7.01–7.04 (dd, 1H, J = 8.8 Hz 2.4 Hz, H-6 coumarin), 7.29–7.40 (m, 5H, Ar–H), 7.71–7.73 (d, 1H, J = 8.8 Hz, H-5 coumarin) 8.38 (t, 1H, J = 5.6 Hz, (C=O)CH_2*NH*); 8.83–8.85 (d, 1H, J = 702 Hz, (C=O)CH*NH*); ^{13}C NMR (100 MHz; DMSO-d_6) δ (ppm): 18.6, 41.7, 52.7, 56.6, 67.5, 102.2, 111.9, 112.9, 114.1, 127.0, 128.1, 128.7, 129.1, 136.6, 153.8, 155.0, 160.5, 161.1, 167.8, 168.9, 171.3; MS (EI, 70 eV) m/z (%): 440 (M^+ + 2, 0.06), 438 (0.65), 378 (14.06), 274 (1.43), 246 (4.88), 189 (7.53), 176 (4.91), 148 (6.42), 106 (100), for $C_{23}H_{27}N_2O_7$ (438.43): calcd% C 63.01, H 5.06, N 6.39; found: % C 63.07, H 5.09, N 6.35.

3.1.14 Methyl2-{2-{2-{2-[(4-methyl-2-oxo-2*H*-chromen-7-yl) oxy]acetamido}acetamido}acetamido} acetate (9a). A white crystals; yield: (80%); mp 175–180 °C $R_f = 0.55$ (2% MeOH/$CHCl_3$); IR ν:(KBr, cm^{-1}): 3293 (NH), 3090 (CH aromatic), 2951 (CH aliphatic), 1742 (C=O, ester), 1647 (C=O, amide), 1607 (C=C), 1557 (C–N); ^{1}H NMR (400 MHz; DMSO-d_6) δ (ppm): 2.40 (s, 3H, H_4–CH_3); 3.63 (s, 3H, O–CH_3); 3.76–3.77 (d, 2H, J = 6 Hz, (C=O)CH_2NH); 3.83–3.85 (m, 4H, 2(C=O)CH_2NH); 4.68 (s, 2H, O–CH_2(C=O); 6.23 (s, 1H, H-3 coumarin)); 7.00 (s, 1H, H-8 coumarin); 7.02–7.05 (dd, 1H, J = 8.4 Hz 2.4 Hz, H-6 coumarin), 7.71–7.73 (d, 1H, J = 8.8 Hz, H-5 coumarin) 8.37 (m, 2H, 2 *NH* (C=O)CH_2); 8.45 (t, 1H, J = 5.6 Hz, (C=O) CH_2*NH*); ^{13}C NMR (100 MHz; DMSO-d_6) δ (ppm): 18.6, 40.9, 42.1, 42.2, 52.1, 67.5, 102.2, 111.9, 112.9, 114.1, 127.0, 153.8, 155.0, 160.5, 161.0, 167.9, 169.3, 169.8, 170.6; MS (EI, 70 eV) m/z (%): 421 (M^+ + 2, 1.95), 419 (29.07), 387 (65.69), 330 (59.51), 274 (100), 246 (98.35), 189 (78.22), 177 (95.15), 148 (44.98), for $C_{19}H_{21}N_3O_8$ (319.39): calcd% C 54.41, H 5.05, N 10.02; found: % C 54.46, H 5.09, N 9.92.

3.1.15 (*R*)-Methyl4-methyl-2-{2-{2-{2-[(4-methyl-2-oxo-2*H*-chromen-7-yl)oxy]acetamido} acetamido}acetamido}pentanoate (9b). A white fine crystals; yield: (82%); mp 76–80 °C; R_f = 0.55 (2% MeOH/$CHCl_3$); IR ν:(KBr, cm^{-1}): 3370 (NH), 3081 (CH aromatic), 2952 (CH aliphatic), 1729 (C=O, ester), 1660 (C=O, amide), 1622 (C=C), 1544 (C–N); ^{1}H NMR (400 MHz; DMSO-d_6) δ (ppm): 0.83–0.89 (dd, 6H, J = 6.4, 12 Hz, $(CH_3)_2$ CH), 1.13 (t, 2H, J = 12 Hz, CHCH_2CH), 1.25 (m, 1H, $(CH_3)_2$ *CH*), 2.41 (s, 3H, H_4–CH_3); 3.61 (s, 3H, O–CH_3), 3.61–3.76 (m, 4H, 2CH_2NH), 4.42 (m, 1H, *CH*NH), 4.67 (s, 2H, O–CH_2(C=O), 6.24 (s, 1H, H-3 coumarin)), 7.00 (s, 1H, H-8 coumarin), 7.01–7.04 (dd, 1H, J = 8.4 Hz 2.4 Hz, H-6 coumarin), 7.71–7.73 (d, 1H, J = 12 Hz, H-5 coumarin), 8.19 (t, 1H, J = 8 Hz, (C=O)CH_2*NH*), 8.37 (d, 1H, J = 6 Hz, (C=O)CH*NH*); 8.44 (t, 1H, J = 5.6 Hz, (C=O)CH_2*NH*); ^{13}C NMR (100 MHz; DMSO-d_6) δ (ppm): 18.6, 21.7, 22.8, 23.1, 24.5, 42.0, 46.0, 50.6, 52.1, 67.5, 102.2, 111.9, 112.9, 114.1, 127.0, 153.8, 155.0, 160.5, 161.0, 167.8, 169.3, 173.3; MS (EI, 70 eV) m/z (%): 477 (M^+ + 2, 0.08), 475 (0.81), 443 (7.22), 416 (9.31), 330 (5.36), 274 (23.46), 246 (20.81), 189 (26.17), 177 (26.36), 148.05 (32.69), 86 (100), for $C_{17}H_{18}N_2O_6$ (475.49): calcd% C 58.10, H 6.15, N 8.84; found: % C 58.15, H 6.12, N 8.81.

3.1.16 (*R*)-methyl2-{2-{2-{2-[(4-methyl-2-oxo-2*H*-chromen-7-yl)oxy]acetamide}acetamide} acetamide}-2-phenylacetate (9c). A white foam; yield: (82%); mp 200–203 °C; R_f = 0.55 (2% MeOH/$CHCl_3$); IR ν:(KBr, cm^{-1}): 3313, 3281 (NH), 3084 (CH aromatic), 2924 (CH aliphatic), 1731 (C=O, ester), 1653 (C=O, amide), 1618 (C=C), 1552 (C–N); ^{1}H NMR (400 MHz; DMSO-d_6) δ (ppm): 2.41 (s, 3H, H_4–CH_3); 3.63 (s, 3H, O–CH_3); 3.81–3.85 (m, 4H, 2CH_2NH); 4.67 (s, 2H, O–CH_2(C=O); 5.43 (d, 1H, J = 7.2 Hz, Ph*CH*NH), 6.24 (s, 1H, H-3 coumarin)); 7.00 (s, 1H, H-8 coumarin); 7.02–7.05 (dd, 1H, J = 8.8 Hz 2.4 Hz, H-6 coumarin), 7.29–7.40 (m, 5H, Ar–H), 7.71–7.73 (d, 1H, J = 8.8 Hz, H-5 coumarin), 8.19 (t, 1H, J = 5.6 Hz, (C=O)CH_2*NH*); 8.43 (t, 1H, J = 5.6 Hz, (C=O)CH_2*NH*); 8.75–8.77 (d, 1H, J = 7.2 Hz, (C=O)CH*NH*); ^{13}C NMR (100 MHz; DMSO-d_6) δ (ppm): 18.6, 41.9, 42.1, 52.7, 56.6, 67.5, 102.2, 111.9, 112.9, 114.1, 127.0, 128.1, 128.7, 129.1, 136.6, 153.8, 155.0, 160.5, 161.0, 167.9, 169.1, 169.2, 171.3; MS (EI, 70 eV) m/z (%): 497 (M^+ + 2, 0.07), 495 (0.16), 463 (13.19), 362 (5.70), 290 (13.27), 274 (15.07), 246 (11.77), 189 (26.38), 176 (14.57), 148 (21.40), 106 (100), for $C_{25}H_{25}N_3O_8$ (495.38): calcd% C 60.60, H 5.09, N 8.48; found: % C 60.64, H 5.06, N 8.42.

3.2. Biological evaluation

3.2.1 *In vitro* anticancer screening. Anticancer activity screening of the synthesized compounds was carried out using reported MTT assay technique.[55] The 96 well tissue culture plate was inoculated with 1×10^5 cells per ml (100 µl per well) and incubated at 37 °C for 24 hours to develop a complete monolayer sheet. Growth medium was decanted from 96 well micro titer plates after confluent sheet of cells were formed, cell monolayer was washed twice with wash media. A two-fold dilution of tested sample was made in RPMI medium with 2% serum (maintenance medium). 0.1 ml of each dilution was tested in different wells leaving 3 wells as control, receiving only maintenance medium. Plate was incubated at 37 °C and examined. Cells were checked for any physical signs of toxicity, *e.g.* partial or complete loss of the monolayer, rounding, shrinkage, or cell granulation. MTT solution was prepared (5 mg ml^{-1} in PBS) (BIO BASIC CANADA INC). 20 µl MTT solutions were added to each well. Place on a shaking table, 150 rpm for 5 minutes, to thoroughly mix the MTT into the media. Incubate (37C, 5% CO_2) for 1–5 hours to allow the MTT to be metabolized. Dump off the media (dry plate on paper towels to remove residue if necessary). Resuspend formazan (MTT metabolic product) in 200 µl DMSO. Place on a shaking table, 150 rpm for 5 minutes, to thoroughly mix the formazan into the solvent. Read optical density at absorbance of 560 nm and subtract background at absorbance of 620 nm. Optical density should be directly correlated with cell quantity. The means of three separate determinations will be reported. Statistical differences were analyzed according to one-way

ANOVA test in which the variance was considered to be significant at $p < 0.05$.

3.2.2 CK2 kinase enzyme inhibitory assay. The CycLex CK2 Kinase Assay/Inhibitor Screening Kit (Catalog CY-1170) was used to carry out the assay. The plates supplied with the kit are precoated with P53 protein which contain serine residue that is phosphorylated by CK2 (Casine kinase 2). Initially, add the kinase solution, and test compound solution, in the presence of the ATP solution into the test wells, and incubate for 30 min at 30 °C. (to let the CK2 phosphorylate the serine residue bound to the plate). End the kinase reaction by adding EDTA solution. Wash the wells by washing buffer then aspirate the residual washing solution. After that pipette HRP conjugated detection monoclonal antibody TK-4D4 to each well (the TK-4D4 detects only the phosphorylated serine residue) and incubate at RT for 30 min. Wash the well with washing buffer and aspirate the residual solution by gentle tapping. Add TMB (the chromogenic substrate of HRP), and incubate at RT for 15 min. The horseradish peroxidase (HRP) catalyzes the conversion of TMS from colorless to blue color that reflects CK2 activity which is measured by spectrophotometer at 450 nm.

3.3. Molecular docking

The new synthesized compounds were subjected to molecular docking in order to recognize their binding modes and free energies of binding towards CK2 receptor. Therefore, crystallographic structure of CK2 receptor in complex with co-crystalized ligand, **G12** was retrieved from Protein Data Bank (PDB ID: 2QC6). The docking analysis was performed using AutoDock program. The 2D chemical structures of the synthesized compounds and co-crystalized ligand were sketched using ChemBioDraw Ultra 14.0. In order to assess the efficacy of the method used for docking, we performed molecular redocking of co-crystalized ligand, **G12** which validated by getting low RMSD values between the docked and X-ray structures. Then the docking of co-crystalized ligand and the synthesized compounds were performed using default protocol parameters. The docking results from AutoDock program was further analyzed and visualized using Pymol software to investigate the putative interaction mechanism with CK2 target. The complexes of synthesized compounds were subjected to energy minimization to optimize the complexes and subsequent MD simulations to predict the energetically most favorable binding mode for the respective compounds and to decrease in the number of false positive and negative docking results. Therefore, the complexes were subjected to MD simulation at 300 K during 400 ps. The time step of the simulation was 2.0 fs with a cutoff 10 Å for the non-bonded interactions. The MD simulation is performed at constant temperature and pressure. During the MD simulation all backbone atoms of the complexes were restrained to their starting positions with harmonic force constant 2.0 kcal (mol^{-1} $Å^{-2}$).

4 Conclusion

Coumarin scaffold have been widely used as an effective template for drug discovery. Thus, a series of novel hybrid coumarin derivatives were designed and chemically synthesized in synthetically useful yields. All the novel synthesized compounds were biologically evaluated *in vitro* for their cytotoxic activities against a panel of three human cancer cell lines, namely HepG-2, PC-3, and HCT-116. The results of cytotoxic estimation indicated that the anticancer activity of the synthesized compounds showed excellent to weak anticancer activity. In particular, compound **7c** appeared to be significantly more potent than doxorubicin with IC_{50} values of 34.07, 16.06, and 16.02 μM against tested cell lines. Furthermore, compound **5b** displayed the highest cytotoxic effect against all tested cell lines with IC_{50} values of 42.16, 59.74, and 35.05 μM compared with an anticancer drug, doxorubicin as a control drug. Besides, compounds **7b**, and **5a** possessed good anti-proliferative activities against the three cell lines with IC_{50} values ranging from 61 μM to 105 μM. Pharmacophoric features indicated that coumarin scaffold having a dipeptide linker substituted with phenyl moiety was more potent than other analogs leading to significant decrease in cytotoxic activity. In addition, the most potent compounds were further evaluated for their activities against CK2 kinase inhibitors. The most potent compound **5b** displayed the most promising inhibitory activity against CK2 kinase with IC_{50} value of 0.117 ± 0.005 μM compared with roscovetine as control drug with IC_{50} value of 0.251 ± 0.011 μM. Finally, molecular docking studies were conducted to explain the anticancer results with the prospective target and the ADME properties were calculated to predict pharmacokinetic and toxic properties of the synthesized compounds.

Data availability

The data supporting this article have been included as part of the ESI.†

Conflicts of interest

The authors declare that they have no known competing financial interests or personal relationships that could have appeared to influence the work reported in this paper.

References

1 M. J. Thun, J. O. DeLancey, M. M. Center, A. Jemal and E. M. Ward, The global burden of cancer: priorities for prevention, *Carcinogenesis*, 2009, **31**, 100–110.
2 S. Yu, Z. Chen, X. Zeng, X. Chen and Z. Gu, Advances in nanomedicine for cancer starvation therapy, *Theranostics*, 2019, **26**, 8026–8047.
3 J. Jampilek, Heterocycles in medicinal chemistry, *Molecules*, 2019, **21**, 3839.
4 A. Stefanachi, F. Leonetti, L. Pisani, M. Catto and A. Carotti, Coumarin: A natural, privileged and versatile scaffold for bioactive compounds, *Molecules*, 2018, **2**, 250.
5 F. Annunziata, C. Pinna, S. Dallavalle, L. Tamborini and A. Pinto, An overview of coumarin as a versatile and readily accessible scaffold with broad-ranging biological activities, *Int. J. Mol. Sci.*, 2020, **13**, 7370201.

6 A.-K. Singh, P. K. Patel, K. Choudhary, J. Joshi, D. Yaday and J. O. Jin, Quercetin and coumarin inhibit dipeptidyl peptidase-IV and exhibits antioxidant properties: *in silico*, *in vitro*, ex vivo, *Biomolecules*, 2020, **2**, 207.

7 G. Wang, Y. Liu, L. Zhang, L. An, R. Chen, Y. Liu, Q. Luo, Y. Li, H. Wang and Y. Xue, Computational study on the antioxidant property of coumarin-fused coumarins, *Food Chem.*, 2020, **340**, 125446.

8 C. T. Supuran, Coumarin carbonic anhydrase inhibitors from natural sources, *J. Enzyme Inhib. Med. Chem.*, 2020, **1**, 1462–1470.

9 D. Cuffaro, E. Nuti and A. Rossello, An overview of carbohydrate-based carbonic anhydrase inhibitors, *J. Enzyme Inhib. Med. Chem.*, 2020, **1**, 1906–1922.

10 R. Nagamallu, B. Srinivasan, M. B. Ningappa and A. K. Kariyappa, Synthesis of novel coumarin appended bis(formylpyrazole) derivatives: studies on their antimicrobial and antioxidant activities, *Bioorg. Med. Chem. Lett.*, 2016, **2**, 690–694.

11 C. Jia, J. Zhang, L. Yu, C. Wang, Y. Yang, X. Rong, K. Xu and M. Chu, Antifungal activity of coumarin against candida albicans is related to apoptosis, *Front. Cell. Infect. Microbiol.*, 2018, **8**, 445.

12 R. Elias, R. I. Benhamou, Q. Z. Jaber, O. Dorot, S. L. Zada, K. Oved, E. Pichinuk and F. Micha, Antifungal activity, mode of action variability, and subcellular distribution of coumarin-based antifungal azoles, *Eur. J. Med. Chem.*, 2019, **179**, 779–790.

13 S. K. Chidambaram, D. Saud-Alarifi, S. Radhakrishnan and I. Akbar, In silico molecular docking: evaluation of coumarin based derivatives against SARS-CoV-2, *J. Infect. Public Health*, 2020, **11**, 1–1677.

14 S. Mishra, A. Pandey and S. Manvanti, Coumarin: an emerging antiviral agent, *Heliyon*, 2000, **1**, e03217.

15 M. Bian, Q. Q. Ma, Y. Wu, H. H. Du and G. Guo-hua, Small molecule compounds with good anti-inflammatory activity reported in the literature from 01/2009 to 05/2021: a review, *J. Enzyme Inhib. Med. Chem.*, 2021, **1**, 2139–2159.

16 H. Yu, Z. Hou, X. Yang, Y. Mou and C. Guo, Design, synthesis, and mechanism of dihydroartemisinin-coumarin hybrids as potential anti-neuroinflammatory agents, *Molecules*, 2019, **9**, 1672.

17 H. W. Querfurth and F. M. Laferla, Alzheimer's disease, *N. Engl. J. Med.*, 2010, **4**, 329–344.

18 M. X. Song and X. Q. Deng, Recent development on triazole nucleus in anticonvulsant compounds: a review, *J. Enzyme Inhib. Med. Chem.*, 2018, **1**, 453–478.

19 C. X. Wei, M. Bian and G. H. Gong, Current research on antiepileptic compounds, *Molecules*, 2015, **11**, 20471–20776.

20 M. Greaves, Pharmacogenetics in the management of coumarin anticoagulant therapy: the way forward or an expensive diversion?, *PLoS Med.*, 2005, **10**, e342.

21 G. Lippi, R. Gosselin and E. J. Favaloro, Current and emerging direct oral anticoagulants state-of-the-art, *Semin. Thromb. Hemostasis*, 2019, **5**, 490–501.

22 A. M. Abu-Odeh and W. H. Talib, Middle east medicinal plants in the treatment of diabetes: a review, *Molecules*, 2021, **3**, 742.

23 Y. Hu, B. Wang, J. Yang, T. Liu, J. Sun and X. Wang, Synthesis and biological evaluation of 3-arylcoumarin derivatives as potential anti-diabetic agents, *J. Enzyme Inhib. Med. Chem.*, 2019, **1**, 15–30.

24 D. Hanahan and R. A. Weinberg, The hallmarks of cancer, *Cell*, 2000, **1**, 57–70.

25 A. Herrera-R, W. Castrillon, E. Otero, E. Ruiz, M. Carda, R. Agut, T. Naranjo, G. Moreno, M. E. Maldonado and W. Cardona-G, Synthesis and antiproliferative activity of 3- and 7-styrylcoumarins, *Med. Chem. Res.*, 2018, **27**, 1893–1905.

26 D. Gupta, S. V. Gupta, K. D. Lee and G. L. Amidon, Chemical and enzymatic stability of amino acid prodrugs containing methoxy, ethoxy and propylene glycol linkers, *Mol. Pharmaceutics*, 2009, **5**, 1604–1611.

27 D. Cao, Z. Liu, P. Verwilst, S. Koo, P. Jangjili, J. S. Kim and W. Lin, Coumarin-based small-molecule fluorescent, *Chem. Rev.*, 2019, **18**, 10403–10519.

28 J. Ge, L. Li and S. Q. Yao, Amino acid that mimics phosphotyrosine, *Chem. Commun.*, 2011, **39**, 10939–10941.

29 Y. L. Lo, C. T. Ho and F. L. Tsai, Inhibit multidrug resistance and induce apoptosis by using glycocholic acid and epirubicin, *Eur. J. Pharm. Sci.*, 2008, **35**, 52–67.

30 F. Chu, X. Xu, G. Li, S. Gu, K. Xu, Y. Gong, B. Xu, M. Wang, H. Zhang, Y. Zhang, P. Wang and H. Lei, Amino acid derivatives of ligustrazine-oleanolic acid as new cytotoxic agents, *Molecules*, 2014, **19**, 18215–18231.

31 C. S. Francisco, L. R. Rodrigues, M. F. S. A. Cerqueira Nuno, M. F. Oliverira-Campo Ana and L. M. Rodrigues, Synthesis of novel benzofurocoumarin analogues and their anti-proliferative effect on human cancer cell lines, *Eur. J. Med. Chem.*, 2012, **47**, 370–376.

32 I. Fotopoulos and D. Hadjipavlou-Litina, Hybrids of coumarin derivatives as potent and multifunctional bioactive agents: a review, *Med. Chem.*, 2020, **3**, 272–306.

33 R. Bhatia and R. K. Rawal, Coumarin hybrids: promising scaffolds in the treatment of breast cancer, *Mini-Rev. Med. Chem.*, 2019, **17**, 1443–1458.

34 A. V. Yurkovetskiy and R. J. Fram, XMT-1001, a novel polymeric camptothecin pro-drug in clinical development for patients with advanced cancer, *Adv. Drug Delivery Rev.*, 2009, **61**, 1193–1202.

35 D. Cao, Y. Liu, W. Yan, C. Wang, P. Bai, T. Wang, M. Tang, X. Wang, Z. Yang, B. Ma, L. Ma, L. Lei, F. Wang, B. Xu, Y. Zhou, T. Yang and L. Chen, Design, synthesis, and evaluation of *in vitro* and *in vivo* anticancer activity of 4-substituted coumarins: a novel class of potent tubulin polymerization, *J. Med. Chem.*, 2016, **12**, 5721–5739.

36 W. Zhang, Z. Li, M. Zhou, F. Wu, X. Hou, H. Luo, H. Liu, X. Han, G. Yan, Z. Ding and R. Li, Synthesis and biological evaluation of 4-(1,2,3-triazol-1-1yl)coumarin derivatives as potential antitumor agents, *Bioorg. Med. Chem. Lett.*, 2014, **3**, 799–807.

37 R. An, Z. Hou, J. T. Li, H. N. Yu, Y. H. Mou and C. Guo, Design, synthesis and biological evaluation of novel 4-substituted coumarin derivatives as antitumor agents, *Molecules*, 2018, **9**, 2281.

38 F. Belluti, G. Fontana, L. D. Bo, N. Carenini, C. Giommarelli and F. Zunino, Design, synthesis and anticancer activities of stilbene-coumarin hybrid compounds: identification of novel proapoptoic agents, *Bioorg. Med. Chem.*, 2010, **10**, 3543–3550.

39 E. H. Maleki, A. Z. Bahrami, H. Sadeghian and M. M. Matin, Discovering the structure activity relationships of different o-prenylated coumarin derivatives as effective anticancer agents in human cervical cancer cells, *Toxicol. In Vitro*, 2020, **63**, 104745.

40 A. Rawat and B. V. A. Reddy, Recent advances on anticancer activity of coumarin derivatives, *Eur. J. Med. Chem.*, 2022, **5**, 100038.

41 A. Herrera-R, W. Castrillón, E. Otero, E. Ruiz, M. Carda, R. Agut, T. Naranjo, G. Moreno and M. E. Maldonado, Cardona-G W. Synthesis and antiproliferative activity of 3- and 7-styrylcoumarins, *Med. Chem. Res.*, 2018, **27**, 1893–1905.

42 Q. P. Diao, H. Guo and G. Q. Wang, Design, Synthesis and *In Vitro* Anticancer Activities of Diethylene Glycol Tethered Isatin-1,2,3-triazole-coumarin Hybrids, *J. Heterocycl. Chem.*, 2019, **56**, 1667–1671.

43 Z. H. Li, X. Q. Liu, P. F. Geng, F. Z. Suo, J. L. Ma, B. Yu, T. Q. Zhao, Z. Q. Zhou, C. X. Huang and Y. C. Zheng, Discovery of [1,2,3]Triazolo[4,5-d]pyrimidine Derivatives as Novel LSD1 Inhibitors, *ACS Med. Chem. Lett.*, 2017, **8**, 384–389.

44 H. Yu, Z. Hou, Y. Tian, Y. Mou and C. Guo, Design, synthesis, cytotoxicity and mechanism of novel dihydroartemisinin-coumarin hybrids as potential anti-cancer agents, *Eur. J. Med. Chem.*, 2018, **151**, 434–449.

45 Z. Xu, X. F. Song, Y. Q. Hu, M. Qiang and Z. S. Lv, Azide-alkyne cycloaddition towards 1*H*-1,2,3-triazole-tethered gatifloxacin and isatin conjugates: Design, synthesis and *in vitro* anti-mycobacterial evaluation, *Eur. J. Med. Chem.*, 2017, **138**, 66–71.

46 B. S. Vig, K. M. Huttunen, K. Laine and J. Rautio, Amino acids as promoities in prodrug design and development, *Adv. Drug Delivery Rev.*, 2013, **65**, 1370–1385.

47 T. Nakanishi, I. Tamai, A. Takaki and A. Tsuji, Cancer cell-targeted drug delivery utilizing oligopeptide transport activity, *Int. J. Cancer*, 2000, **88**, 274–280.

48 X. Song, P. L. Lorenzi, C. P. Landowski, B. S. Vig, J. M. Hilfinger and G. L. Amidon, Amino acid ester prodrug of the anticancer agent gemcitabine: Synthesis, bioconversion, metabolic bioevasion and hPEPT1-mediated transport, *Mol. Pharm.*, 2005, **2**, 157–167.

49 A. Lacy and R. O. Kennedy, Studies on coumarins and coumarin-related compounds to determine their therapeutic role in the treatment of cancer, *Curr. Pharm. Des.*, 2004, **30**, 3797–37811.

50 A. Chilin, R. Battistutta, A. Bortolato, G. Cozza, S. Zanatta, G. Poletto, M. Mazzorana, G. Zagotto, E. Uriarte, A. Guiotto, L. A. Pinna, F. Meggio and S. Moro, Coumarin as attractive casein kinase 2 (CK2) inhibitors scaffold: an integrate approach to elucidate the putative binding motif and explain structure activity relationships, *J. Med. Chem.*, 2008, **4**, 752–759.

51 N. Zhang and R. Zhong, Docking and 3D-QSAR studies of 7-hydroxycoumarin derivatives as CK2 inhibitors, *Eur. J. Med. Chem.*, 2010, **1**, 292–297.

52 V. S. V. Satyanarayana, P. Sreevani, A. Sivakumar and V. Vijayakumar, Synthesis and antimicrobial activity of new Schiff bases containing coumarin moiety and their spectral characterization, *ARKIVOC*, 2008, **17**, 221–233.

53 K. A. Alheety, N. M. Jamel and B. J. Ahmed, Synthesis of coumarin by Pechman reaction a review, *J. Pharm. Sci. Res.*, 2019, **9**, 3344–3347.

54 A. H. Abdel-Rahman, W. A. El-Sayed, H. M. Abdel-Bary, A. S. Abdel-Megied and M. I. Morcy, Amino acid derivatives, VIII [1]: synthesis and antimicrobial evaluation of alpha-amino acid esters bearing an indole side chain, *Monatsh. Chem.*, 2008, **139**, 1095–1101.

55 J. Van Meerloo, G. J. Kaspers and J. Cloos, Cell sensitivity assays: the MTT assay, *Methods Mol. Biol.*, 2011, **731**, 237–245.

56 C. Borgo and M. Ruzzene, Role of protein kinase CK2 in antitumor drug resistance, *J. Exp. Clin. Cancer Res.*, 2019, **38**, 287.

57 N. Zhang, W. J. Chen, Y. Zhou, H. Zhao and R. G. Zhong, Rational design of coumarin derivatives as CK2 inhibitors by improving the interaction with the hinge region, *Mol. Inf.*, 2016, **35**, 15–18.

58 N. Zhang and R. Zhong, Docking and 3D-QSAR studies of 7-hydroxycoumarin derivatives as CK2 inhibitors, *Eur. J. Med. Chem.*, 2010, **45**, 292–297.

59 J. E. Chojnowski, E. A. McMillan and T. Strohlic, Identification of novel CK2 kinase substrates using a versatile biochemical approach, *J. Visualized Exp.*, 2019, **21**, 59037.

60 L. Meijer and E. Raymond, Roscovitine and other purines as kinase inhibitors from starfish oocytes to clinical trials, *Acc. Chem. Res.*, 2003, **36**, 417–425.

61 C. Borgo and M. Ruzzene, Role of protin kinase CK2 in antitumor drug resistanc, *J. Exp. Clin. Cancer Res.*, 2019, **38**, 287.

62 B. Guerra and O.-G. Issinger, Role of protein kinase CK2 in aberrant lipid metabolism in cancer, *Pharmaceuticals*, 2020, **13**(10), 292.

63 G. Loele, M. Chieffallo, M. A. Occhiuzzi, M. D. Luca, A. Garofalo, G. Ragno and F. Grande, Anticancer drugs: recent strategies to improve stability profile, pharmacokinetic and pharmacodynamics properties, *Molecules*, 2022, **27**, 5436.

64 Small-Molecule Drug Discovery Suite, *QikProp, Version 4.2*, New York, Schrodinger, LLC, 2014.

65 C. M. Chagas, S. Moss and L. Alisaraie, Drug metabolites and their effects on the development of adverse reactions: revisiting Lipinski's Rule of five, *Int. J. Pharm.*, 2018, **549**, 133–149.

66 M. D. Naik, Y. D. Bodke, K. M. Vijay and B. C. Revanasiddappa, An efficient one-pot synthesis of coumarin-amino acid derivatives as potential anti-inflammatory and anti-oxidant agents. Syn, *Commun*, 2020, 1735442.

67 B. L. Sousa, P. V. Leite, A. O. Mendes, V. V. Varejao, C. S. Chaves, J. G. Silva, A. P. Agrizzi, P. G. Ferreira, E. J. Pilau, E. Silva and M. H. Santos, Inhibition of acetylcholinesterase by cumarin-linked amino acids synthetized *via* triazole associated with molecule partition coefficient, *J. Braz. Chem. Soc.*, 2021, **32**, 652–664.

68 M. S. Gomaa, I. A. I. Ali, G. El Enany, E. H. El Ashry, S. M. El Rayes, W. Fathalla, A. H. A. Ahmed, S. A. Abushait, H. A. Abushait and M. S. Nafie, Facile synthesis of some coumarin derivatives and their cytotoxicity through VEGFR2 and topoisomerase II inhibition, *Molecules*, 2022, **27**, 8279.

69 V. F. Morales, A. P. Villasana-Ruiz, I. G. Veloz, S. G. Delgado and M. L. Martinez-Fierro, Theraspeutic effects of coumarins with different substitution patterns, *Molecules*, 2023, **28**, 2413.

70 M. Koley, J. Han, V. A. Soloshonok, S. Mojumdr, R. Javahershenas and A. Makarem, Latest developments in coumarin-based anticancer agents: mechanism of action and structure-activity relationship studies, *RSC Med. Chem.*, 2024, **15**, 10–54.

71 V. S. V. Satyanarayana, P. Sreevani, A. Sivakumar and V. Vijayakumar, Synthesis and antimicrobial activity of new Schiff bases containing coumarin moiety and their spectral characterization, *Arkivoc*, 2008, **17**, 221–233.